arXiv:astro-ph/0201135v2 11 Jan 2002

THE PHOTOMETRIC AND SPECTRAL INVESTIGATION OF CI CAMELOPARDALIS, AN X-RAY TRANSIENT AND B[e] STAR

E.A.Barsukova[1], N.V.Borisov[1],V.P.Goranskij[2], V.M.Lyuty[2], and N.V.Metlova[2].

[1] Special Astrophysical Observatory, Russian Academy of Sciences, Nizhny Arkhys, Karachaevo-Cherkesia, Russia

[2] Sternberg Astronomical Institute, Moscow University, Russia

Key words: X-ray binaries, microquasars, photometry, spectroscopy.

We combined the results of $UBVR$ photometry of CI Cam taken at Sternberg Astronomical Institute in 1998–2001, and moderate resolution spectroscopy taken at Special Astrophysical Observatory during the same time period. Photometry as well as fluxes of Balmer emissions and of some Fe II emission lines of CI Cam in quiet state reveal a cyclic variation with the period of 1100 ± 50^d. The variation like this may be due to an orbital motion in a wide pair with a giant star companion that exhibits the reflection effect on its side faced to a compact companion.

The V-band photometry also confirms the pre-outburst 11.7 day period found by Miroshnichenko earlier, but with a lower amplitude of 3 per cent. The possibility of identity of this photometric period with the period of jet's rotation in the VLA radio map of the object CI Cam was investigated. The radio map modelling reveals the inclination of the jet rotation axis to the line of sight, $i = 35 - 40^o$, the angle between the rotation axis and the direction of ejection of the jet, $\theta = 7 - 10^o$, and jet's spatial velocity of 0.23–0.26c.

Equivalent widths and fluxes of various spectral lines show different amplitudes of changes during the outburst, and essentially distinct behaviour in quiescence. Five types of such behaviour were revealed, that indicates the strong stratification of a gas and dust envelope round the system . The time lag of strengthening of 50–250^d in the forbidden line of nitrogen [N II] was found relatively to the X-ray outburst maximum.

Introduction

CI Cam (MWC 84, KPD 0415+5552, MW 143, LS V $+55^o16$, IRAS 04156+5552, XTE J0421+560; $4^h19^m42^s.11$, $+55^o59'57''.7$, 2000) is a well-known B[e] star, $V = 11^m.6$, an X-ray system, and a microquasar. Stars having the following spectral features are usually attributed to B[e] star class [1]: (1) bright hydrogen and helium emissions above the blue continuum; (2) numerous bright lines of Fe II and other metals, mainly at low ionization levels and with low excitation potential; (3) forbidden emission lines of metals and of other elements in optical spectrum, e. g. [Fe II], [O I]; (4) strong infrared excess due to radiation of hot circumstellar dust. CI Cam does have these features in its spectrum. Since 1932, it is known as a B star with H_α, He I and Fe II emissions [2,3]. The spectrum of the star was thoroughly studied in [4,5]. The results of broad-band photometry in optical and infrared diapasons are presented in [6]. The star showed a significant light variability with the amplitude up to $0^m.4$ in the V band, and therefore was included into General Catalogue of Variable Stars. The photometric 11.7 day period was determined in [5,7] based on data [6], the amplitude of periodic component being $0^m.3$ V. The sum of two spectra B0V + G8II [7], or B0V + K0II [5] fits the spectral energy distribution of this system. The observation of absorption lines from a cool star is even reported in [5]. Thus, CI Cam resembles symbiotic variable stars, which have properties overlapping largely with the B[e]-stars ones. The light of star is considerably absorbed. The significant part of this absorption has a circumstellar origin. The star's distance is of 1 kpc [8].

In 1998, April the star underwent a powerful X-ray outburst, its 2–12 KeV flux reached 2 Crabs at maximum on April 1, 0^h57^mUT (JD 2450904.54). The X-ray flux raise to maximum lasted for a few hours [9]. The posterior fading was violent, too, the first two days the flux decreased with the parameter $\tau_e = 0^d.56$ (τ_e is the time of fading by e times). The rate of fading on the 4-th day was in accordance with $\tau_e = 2^d.34$ (slowing down of fading). The X-ray spectrum was soft relative to X-ray novae, and did not expand in the energy range above 60 KeV [10]. The following emissions were seen: the K line of Fe XXV–Fe XXVI at 6.4–6.9 KeV, S XV–S XVI at 2.45–2.62 KeV, and the L line of Si XIII-Si XIV at 1.86–2.01 KeV [11].

Optical observations were carried out with some delay relatively to the X-ray maximum, which is necessary for identification. The greatest brightness registered in the outburst was 7.1 R [12]. Considerable brightening of emission lines occured in optical and infrared spectra [13,14], and the

strong He II 4686 Å emission appeared [13]. H and He emissions had wide pedestals showing the expansion velocity of 1200 km/s in the star envelope [15]. The contribution of emission lines to photometric bands increased. Radio source was detected by April 1, and got maximum of 120 mJy at 1.4 GHz on April 3.83 UT. The radio flux curves, as well as those of X-ray, optical, and infrared fluxes versus time were published in [16]. The time delay of the outburst maximum depending on the increasing of radiation wavelength was noticeable in radio. The rate of optical brightness decline was $\tau_e = 3^d.4 \pm 0^d.4$ since April 3 to April 19, 1998.

The radio source is a syncrotron source by nature. On April 5 it was resolved into a central core and opposite directed jets, which got later S-shaped appearence similar to the radio jets of SS 433. The radio map was published in [17]. The proper motion of each jet was 26 milliarcseconds per day, or $0.15c$ assuming the distance of 1 kpc [18]. A structure of jets is symmertic, and they are corkscrewing along a conic surface. As a galactic stellar system with jets, CI Cam entered the class of objects called "microquasars".

The X-ray flux had declined down to the detectable level in 10–15 days after peak of the outburst. An increased brightness in the optical range was observed till the end of observing season at JD 2450941 (37^d), but it got the low level in the beginning of the next season at JD 2451051 having later the tendency of brightening [16]. At the same time the radio flux was measurable during all the next season JD 2451020-51300 with tendency of decline [16]. The object was detected in X-rays with BeppoSAX satellite in the quiescence using long exposures with soft spectrum on JD 2451425 [19], or hard spectrum on JD 2451445 [20], or not detected at all. These observations reveal the variability of the object at least by order of magnitude. Spectral study of CI Cam in December 1998 and January 1999 [19] showed no spectral changes during that time period and similarity to the pre-outburst spectrum [4].

This paper presents the results of our photometric and spectral monitoring of CI Cam in quiescence in 1998–2001, and the comparison of photometrically calibrated spectra taken in outburst of 1998 and in quiescence.

Photometric observations

Photometric observations began on 1998 April 3 as soon as we had received the information about the outburst. The observations were carried out with SBIG ST-6 CCD at 60-cm Zeiss reflector of the Sternberg Institute's

Crimean Laboratory. The monitoring was continued during 3 years by N.V. Metlova with the same telescope and one-channel UBV-photometer constructed by V.M. Lyuty. The comparison star GSC 3723.54 ($V = 10^m.401$; $B - V = 0^m.759; U - B = 0^m.336$) and the check star GSC 3723.104 ($V = 12^m.386$; $B - V = 0^m.617; U - B = 0^m.408$) were photometrically calibrated relative to North Polar Sequence (NPS).

During the season of 1998–1999 the photoelectric BVR observations were carried out with 70-cm reflector of the Sternberg Institute in Moscow with one-channel photometer constructed by I.M. Volkov and S.Yu. Shugarov. The photomultiplier FEU-79 was used to repeat the response close to that of Johnson's R_J band. The BVR magnitudes of the same reference stars were measured relative to stars of catalogue [21]. The B and V magnitudes of reference stars were found to be close to previously determined ones within the limits of few hundredth of magnitude, and the R magnitudes were $9^m.884$ and $12^m.034$, accordingly for comparison and check stars. The characteristic accuracy of a single measurement was of $0^m.02 - 0^m.03$.

In 2001 January we took a set of CCD observations in BVR bands with K585 CCD (530x590 pxl) made by scientific and industrial group 'Electron', using 1-m Zeiss reflector of SAO RAN. The comparison star GSC 3723.104 situated within the field of the frames was used. The preliminary reduction were carried out in the MIDAS environment taking into account the frames of bias, dark and flat. Our photometry was performed with a V.P. Goranskij's software based on the method of corrected aperture measurements and operating in OS Windows NT. The results agree well with the photoelectric photometry, but have a higher accuracy of $0^m.005$ in V and R bands. We have carried out monitoring in B band continued for 27^m and 28^m in two nights on JD 2451928 and 2451929 with 40^s exposures. The dispersion of measurements was $0^m.008$ and $0^m.007$ for these nights, accordingly. Such a small dispersion confirmed the complete absence of rapid variability within the scale of minutes and tens of minutes or flickering characteristic of some symbiotic variables.

Additionally, the published data in $UBVR$ bands from [16,19,22,23] were used for our analysis. The systematic differences between the individual observing sets of UBV bands were determined using simultaneous or close by time observations, and these differences were taken into consideration in the way to reduce all the data to a single homogeneous Crimean set obtained by N.V. Metlova. The results of our observations are collected in Table 1, and the light curves in quiescence are shown in Fig. 1.

The cycle of sinusoidal light variation is seen in Fig. 1 in all the bands with the amplitudes of $0^m.2U$, $0^m.15B$ and $0^m.12V$, with a broad brightness maximum around JD 2451270, and the more narrow minimum around JD 2451820. The duration of the cycle is $1100^d \pm 50^d$. The dispersion of the V light curve is very small, it is only of $0^m.029$. The behaviour of the star after the outburst differs radically from that one observed before the outburst as appears from observations [6], although at an average the levels of brightness have not changed in quiescence. Our data show a clear correlation of brightness changes in all the bands. For instance, the correlation coefficient between B and V is equal to 0.84, and that between U and B is equal to 0.82. These coefficients are equal only to 0.58 and 0.37, correspondingly, for observations in [6]. Probably, the observations in [6] have a lower accuracy. Such a cyclic behaviour of the star after its outburst resembles that of some symbiotic stars revealing the periodic variability due to the reflection effect. In such cases, the period of variability coincides usually with the orbital period.

To verify the $11^d.7$ day period found by Miroshnichenko [5] in the observations from [6] with our photometry, at first, we substracted the mean smoothed light curve of the 1100^d cycle from all UBV band light curves. This procedure called prewhitening is widely used in the frequency analysis. Then the residuals were subjected to frequency analysis, making use of Deeming [24] method. The period by Miroshnichenko may be confirmed only by our V band observations. The dispersion of the residuals is only $0^m.029$ in this band. The amplitude spectrum of the harmonic component is shown in Fig. 2. The estimates of significance levels for the peaks in the spectrum are revealed from the analysis of the amplitude distribution function of random series calculated from the initial series of residuals by shuffling among its magnitudes. The amplitude of the peak concerning to the 11-day period is equal only to $0^m.015$. The light curve is shown in Fig. 3. The significance level of this period is very high and exceeds the value of 99.999%, inspite of the fact that the amplitude of our light curve ($0^m.03$) is at least 5 times less then that one in [5]. The dispersion of our light curve is $0^m.024$, so the conribution of the periodic component to the residuals is only ≈20 per cent. The phases of the light curve given in Fig. 3 are calculated with the formula:

$Max = 2451075.56 + 11^d.719 \cdot E$ (1).

The value of period has been defined with the accuracy of $\pm 0^d.02$. Undoubtedly the period is real due to coincidence with the value found by Miroshnichenko with the independent set of data, although no significant

peaks have been found in the frequency spectra of B and U band data. It is assumed that the observations in V band are more accurate than in other bands. Using again the photometry published in [6], we have revealed the following formula valid before the outburst:

$Max = 2448995.64 + 11^d.704 \cdot E \qquad (2).$

Here, the period value may be defined in the range from $11^d.69$ to $11^d.72$. Then the amplitude of the periodic component in the light curve was $0^m.16$ B, $0^m.13$ V and $0^m.10$ R. The shape of the light curve in B and R bands was close to a sinusoid. It is two-humped in V band (see Fig. 4 in [5]). Phases calculated with formulae (1) and (2) do not agree, but the agreement of light curves before the outburst and after it may be achieved with two alternative period values $11^d.69$ and $11^d.75$. It should be noted, that in [25] the $11^d.7$ period was not confirmed with CCD photometry in 1999.

We have studied the possibility of connection between the photometric 11-day period and the period of jet rotation observed by methods of radio interferometry. The VLA radio map of CI Cam was published in [17]. The date of this map is not given, but its dimensions are 0.6x0.6 arcseconds. Two opposite S-shaped jets are seen in the map, the size of each one reaches $0''.3$, measuring from the central source. The structure corresponds approximately to a single revolution of corkscrewing spiral located in a conic surface. If we adopt the proper motion of each jet of 0.026 arcseconds per day from [18], we will get the time of a single revolution of $11^d.5 \pm 1^d.0$, which is very close to the value of period by Miroshnichenko. If connection between radio and optical periods exists, the 11-day period may be treated as the rotation period of the star with a dipole magnetic field, the axis of the magnetic dipole inclining to the axis of rotation, and with jets to be ejected just along the axis of the magnetic dipole.

The model of rotating jets was constructed to verify this hypothesis. A computer software created earlier to calculate the structure of SS 433 jet was used. Four parameters were searched to describe the shape of jets seen in the radio map [17]: i is the inclination angle between the axis of star rotation and the line of sight, θ is the angle between the rotation axis and the direction of the jet outflow, ψ is the rotation phase of the moment when the jet outflow had begun, and the fourth parameter is the date of the radio map. ψ parameter is an analogue of the precession phase for the jet of SS 433. It is counted out from the moment when the angle between the jet and the line of sight was minimum. According to our hypothesis, just this moment the brightness of the rotating star had to be the highest

one. The rotation period was assumed to be equal to $11^d.7$.

The narrow ranges of the angles $i = (35 - 40^o)$ and $\theta = (7 - 10^o)$ were found as a result of the modelling. Using these angles, we have calculated the real velocity of jets in space which is equal to 0.23–0.26c, if the projection of this velocity on the plane of the sky is 0.15c [18]. One may consider 1998 March 31.6 UT (JD 2450904.1), when the X-ray outburst has started [9], as the start of jet outflow. The calculated rotation phase ψ of the outflow start depends on what the fraction of jet revolution occured by the moment of taking the radio map, and therefore on the date of this map. The radio map may be reproduced by our model already at 78 per cent of the jet revolution, that corresponds to a minimum date of 1998 April 9.4 UT and to $\psi = 0.69$. A complete revolution would correspond to date of 1998 April 12.6 UT and to $\psi = 0.74$. The inclination angle i may be determined up to its sign, and the ψ phase may have additional values in the range of the $\psi = 0.19 - 0.24$ due to the uncertainty of choice of the jet directed toward the observer. The calculated ψ phases of the X-ray outburst start are 0.37 from formula (1), and 0.06 from formula (2), and both do not agree with the calculated ranges of the ψ parameter.

The main conclusion of our modelling of jets is that the radio map [18] may be represented by the model of jets rotating with the 11.7-day period using a specific set of parameters. Moreover, the modelling may relate the appearence of the jet with the phase of the 11-day period light curve. This will become possible after publication of VLA radio maps with the specific dates of observations, and after a correction of 11-day period.

Spectral observations

Spectral observations of CI Cam began with the 6-m BTA telescope at the outburst on 1998 April 4 using the SP-124 spectrograph, and continued till 2001 January 27 mainly with 1-m Zeiss reflector of SAO and the UAGS spectrograph. The spectra were registered with different CCDs. The primary reduction was made in MIDAS environment taking into account the frames of bias and darkness. All the spectra taken during individual nights were put together. They were calibrated to wavelength scale with the reference spectra of Ne-Ar lamp. The sky background was exposed through the same slit as a star from opposite sides of star spectrum, it was summed up by frame rows, and then subtracted from star spectrum. A series of spectra on 2000 December 6 was not taken with a slit, but taken with an aperture, and the night sky spectrum was not exposed separately. These

spectra were used only to measure the radial velocity. Finally, all spectra were normalized to continuum, the value of which was accepted as a unit. All spectral reductions were performed by E.A. Barsukova. A total list of spectra along with their dates, spectral range and resolution, number of frames per night, lists of telescopes and of observers are given in Table 2.

The results of our spectral observations in the outburst were published partly in [13,15].

A typical spectrum in quiescence is shown in Fig. 4a, 4b. It repeats in detail the spectrum before the outburst published by Downes [4], and that one after the outburst published by Orlandini et al. [19]. The line identification is given in the figure. We used literature sources of spectroscopic data and laboratory wavelengths of emission lines from [26–29]. The bright Balmer emissions, the emissions of neutral helium, the numerous permitted iron lines, as well as a weak silicon line at λ 6347Å, and a forbidden emission of nitrogen are seen in this spectrum. Without any doubt, we identify the emission at λ5755Å as a forbidden line of nitrogen [N II] as distinct from the identification with Fe II in [4] and [19]. So, the difference between the wavelength of this line and laboratory one by 8Å noted in [19] is due to misidentification. We did not find any enough bright forbidden line of [Fe II] in our spectral range; in particular, we identified the emission at $\lambda \approx$ 4416Å as Fe II λ 4414.78Å as distinct from [Fe II] in [19]. Thus, because of the absence of [Fe II] lines in the optical spectrum of CI Cam, the star does not correspond with the canonic description of B[e] star class in one of its aspects.

At first sight, it is difficult to notice the difference between the spectra in quescence and ones in outburst (see e.g. [13, 15]). The set of lines remained the same, they only changed their relative brightness. The most noticeable spectral changes in the outburst are the following. The wide pedestals appeared during the outburst in Balmer and He I lines which are evidence of the motions of matter with velocities up to 1200 km/s, although narrow components of profiles 200–400 km/s wide seen in quescence remained, too. A bright emission of He II λ4686Å emerged. This emission is very weak but measurable in quiescence. The bright emission of Na I D_1 and D_2 doublet appeared as well, it merging with wide He I λ 5876Å line, and looking like a hump in its profile. As the brightness declined, and width of He I line decreased, the sodium emission got detached from the helium line, and vanished then. It has a complicated profile in the high resolution spectrum, containing emission and absorption components, clearly the last ones have interstellar origin. On the contrary, the forbidden line of [N II]

λ 5755Å almost invisible during the outburst, became one of the brightest lines after the outburst. Note that this line was seen before the outburst ([4], marked as Fe II), having the same brightness as after the outburst.

The contribution of the emission lines to the broad B and V bands (of the $UBVR_J$ photometric system) is ≈10 per cent in quiescence and ≈40 per cent in outburst, but it is respectively of 38 and 58 per cent to R_J band, which the very bright emission of H_α is located in.

(a) Equivalent widths and fluxes of emission lines

The equivalent widths of bright emission lines marked with filled squares in Fig. 4a, 4b were measured, and then were re-counted into fluxes in physical quantities of $erg/cm^2/s$ with the help of the photometric data. Mainly the brightest lines were chosen, not the blends. In some cases when a line proved to be a blend and could not be resolved, the total equivalent width of components was measured. Additionally the ratios of outburst-to-quiescence values were determined for both equivalent widths, and fluxes. Mean values of first two nights of observations on April 4 and 5 were adopted as a characteristics of outburst, because the observations had not been carried in the peak of outburst. Mean values for the following observing season of 1999 were adopted as a characteristics of quiescence. The results of observations as ratios of equivalent widths, logarithms of flux ratios, as well as logarithms of total excitation potentials (sum of ionization potential and excitation potential, from [27]) of each line are collected in Table 3.

The typical relations of equivalent widths versus time are shown in Fig. 5. There, the observations by Orlandini et al. [19] are marked with open circles, our ones are marked with filled circles. The equivalent width measurements from [19] agree well with ours, what cannot be said about line fluxes. Probably, the considerable systematic difference in photometry is a cause of disagreement. The typical relations of line fluxes versus time are shown in Fig. 6. The run of parameters in the course of the outburst in 1998 is not shown in Fig. 5 and 6, for better imaging of the quiescent behaviour. Only the final stage of the outburst decay is seen in the most of plots. The scales of line variations in outburst may be estimated with the data of Table 3. Various lines show essentially distinct behaviour. One may distinguish at least 5 types of spectral line behaviour, these types are given in the last column of Table 3.

The He II type

A strong outburst of the emission with equivalent width variation at least of 133 times, and flux variation of 300 times relative to quiescence occured. It is not shown in the figure due to inconvenience of presentation. Probably, the He II line originated in immediate vicinity of the compact object.

The Hα type

The line flux outburst by 5–10 times was observed, then sinusoidal change of equivalent width reproduced the cycle of brightness variability in detail (Fig. 5a). The correlation between equivalent widths of lines of this type and brightness in $UBVR$ bands exists. Balmer lines, and a majority of Fe II lines vary in such a way. The equivalent width variations of these lines do independently confirm the photometric 1100-day cycle. As a result of conversion of equivalent widths to fluxes, the relative amplitude of cyclic variation increases from 25 to 43 per cent (see Fig. 6, H_β). Undoubtedly, the part of Balmer emission belongs to gaseous envelope of the system. Probably, once more region of this type line formation exists on the part of the normal star surfice faced to the compact companion, nearby the interior Lagrangian point L_1. It is just the region which may be responsible for the line brightness variations with the phase of the orbital period.

The He I type

The line flux outburst by 15–50 times took place, then strong irregular changes of equivalent widths were detected in quiescence (Fig. 5b). Besides all He I lines, two lines of the Fe II λ 6318 and 6385Å belong to this type. Cyclic 1100-day variation was not observed. The lines of He I type showed gradual systematic weakening of the flux and the equivalent widths in the season of 1999 (JD 2451399–2451485), when the H_α type lines had a wide maximum of the dependence of equivalent widths upon time. Note that the X-ray source was detected with BeppoSAX sattelite having a soft spectrum in the beginning of this season, and later having a hard spectrum in the middle of the season [19, 20]. Probably, the behaviour of such type lines is sensitive to the X-ray flux from the compact companion, and we have observed the decay of line fluxes after a weak local X-ray flare. So, the He I type lines may be formed close to the compact companion, possibly, in the accretion disk.

The Si II type

The line intensity outburst by 6-18 times was followed by a gradual slow decay of the brightness. No trace of cyclic 1100-day variation is apparently observed. Besides the Si II λ6347Å two line of Fe II λ6148 and 6492Å vary

in such a way (see Fig. 5c, three lower curves).

The [N II] type

The [N II] λ5755Å line finds itself both in the blue and in the red spectra, therefore its variation has been traced in more detail (Fig. 5c, the upper curve). The emission was very weak but measurable during the outburst, and its equivalent width was gradually increasing in the course of star brightness decay (Fig. 5c, the upper curve). It reached maximum in the end of the outburst, and then decreased gradually. Nevertheless, the flux in this line was constant in the outburst during 50 days, but in 250 days after the X-ray peak it increased by one and a half times. That time all other line fluxes had already decreased to their quiescent levels. Later, by the beginning of 2001 the flux of the [N II] line fell down to its outburst level.

This forbidden line usually forms in the most rarefied medium, which can exist only in the exterior edge of so dense gas and dust envelope as that observed for CI Cam. If we assume that the line brightening is caused by the outburst radiation wave arriving at outlying parts of the envelope, than the exterior envelope radius shoud be equal to *at least* 50 light days, what is of $5 - 8''$ for the known distance to the star. No nebulosity is observed on the deep limiting frames taken with broad band filters. The profiles of brightness distribution measured accurately along the slit of our spectra from 6-m telescope with angular resolutions of 2–3 arcseconds both in the [N II] λ5755Å emission and in the continuum do not differ absolutely, the FWHM coinciding with the accuracy of 3–5 per cent! So, the above assumption can not be accepted.

An alternative assumption is that the emission's brightening in 50 – 250 days after the outburst is caused by ejection of rarefied matter beyond the envelope range when some density wave generated by the outburst reaches to the exterior edge of the envelope. The velocity of wave motion may be derived as 1200 km/s using pedestal widths of emission lines during the outburst [15, 23]. Then the outer radius of envelope should be at least $0''.02 - 0''.03$ what is beyond the limit of accuracy of our along slit spectra measurements . Gaseous medium with the density of $10^5 - 10^6$ atoms/cm^3 may extend up to this distance.

The existence of five types of spectral line behaviour confirms that a stratified envelope exists in the system. The H_α type of a cyclic 1100-day variation of equivalent width of some lines indicates the presence of a giant star in the system, this giant having the reflection effect on the region of its surface faced to the compact object. The relation between the line flux

outburst-to-quiescence ratio and the total line excitation potential is shown in Fig. 8 in logarithmic scale. The clear dependence between the outburst amplitude and the excitation potential confirms the envelope stratification; in the envelope the closer the location of radiation source and the stronger the source, the higher excited and ionized matter is.

(b) Radial velocities

In the course of radial velocity calibration of spectra with the UAGS spectrograph of the 1-m Zeiss telescope we have found the sighificant systematic errors of the dispersion curves changing from night to night by 2–3Å. Probably, they are due to device bending. Nevertheless, the internal accuracy of dispersion curve approximation is always equal to 0.2–0.4Å, or 10–20 km/s in the velocity scale. To minimize systematic errors of our radial velocities we referred the velocity scale to telluric lines. The bright sky line of [O I] λ5577Å was used in the blue spectra, and the head of O_2 λ6872Å atmospheric absorption band was used in the red ones. This band does not split into components at our spectral resolution, seems symmetric enough, and may be a good bench mark. The systematic difference of radial velocity level between blue and red parts of spectra may be caused by uncertainty of the effective wavelength of the O_2 band. Both the line of sky and the absorption band are well seen in all the spectra. In such a way we have obtained the uniform sets of radial velocities for H_α, [N II] λ 5755Å and for several Fe II and He I lines, closely spaced in the spectra to selected reference lines. The BTA spectrograms were referred in the same way to reach a homogeneity. The radial velocity curves of selected lines are shown in Fig. 7.

H_α line and Fe II λ5535 and 6516Å lines do not show any changes of radial velocity, including the time of outburst. It is clear if the source of line radiation is located close to inner Lagrangian point, i.e. close to the mass center of the system. It should be noted that amplitudes of component velocities are expected to be small in the system having so long orbital period, as 1100 days. The small radial velocity variations from season to season are visible in the He I λ6678 and 7065Å lines, and a systematic velocity directed to the observer of 50–100 km/s is noticeable during the outburst. This systematic velocity in outburst may be due to partial screening of the red part of the line profiles by matter in the disk plane inclined to the line of sight. The same but oppositely directed systematic velocity is seen in the Fe II λ5362Å line at the time of the

outburst. The forbidden [N II] λ5755Å line also has a positive velocity deviation during the season of the most brightness. Probably, these lines are forming far from the accretion disk, and therefore they behave otherwise than He I lines. Our observations give hope that the orbital motion in CI Cam may by detected in some lines (He I, for instance) using moderate resolution spectra. Additional observations at least of one more possible orbital cycle are needed.

Summary and conclusions

On the grounds of photometry and spectroscopy, some details of conception appear that CI Cam is a stellar system with the orbital period of 1100 days consisting of a giant star and a compact object. The high temperature continuum may belong to an accretion disk or to matter surrounding the compact object. The system is imbedded in a dence and strongly stratified gas and dust envelope, and resembles symbiotic systems. A part of the giant star surface is heated in the region of the inner Lagrangian point, and the reflection effect is in action (at least now). Probably, the giant is a late spectral type one, G8II–K0II [5, 7].

The compact object may be a star having a strong magnetic field, the dipole axis of which is inclined to the rotation axis, and the rotation period may be of 11.72 days. In quiescence, an accretion on the compact object from the dence circumstellar medium goes along the lines of the magnetic field, so we observe hot spots or accretive columns in the poles of the dipole like those in polars, dwarf stellar systems. The contribution of the hot spots to the common light is small, and the variability amplitude due to the compact object rotation is small, only about 3 per cent in V, and less in other bands. But it might be 5 times larger before the outburst according to Miroshnichenko [5]. In outburst ionized matter modifies the magnetic field structure. The plasma accelerates along the curve dipole lines up to relativistic velocities ($\approx 0.25c$). Coriolis forces exert considerable pressure upon the lines of the magnetic field, and as a result the magnetic field lines are rolled up into a collimated tube. This phenomenon may be a jet collimation mechanism. The syncrotron radio emission of jets is evidence that the jet's plasma moves in a strong magnetic field.

Of course, new additional observations and theoretical calculations are needed to confirm and specify this conception. So, accurate photometry and medium-resolution spectroscopy during at least one more 1100-day cycle are able to show if this cycle of variability reflects the real orbital

period. An analysis of original date-fixed VLA radio maps and of accurate photometry may give a more precise picture of jet outflow and clarify a mechanism of an ejection for collimated jets.

The assumption about a white dwarf and a thermonuclear explosion of matter supplied on its surfice due to accretion has the most grounds to explain the nature of the compact object and the outburst in April, 1998. The white dwarf hypothesis is based on the following arguments [19]. First, the two-temperature termal X-ray spectrum in the outburst, and an outburst duration of about a week being in agreement with Iben's calculation [30] of a thermonuclear runaway on the surface of a hot white dwarf with of $\approx 1\ M_\odot$ mass. [At the same time no X-ray flux is usually observed in analogous situation in the Novae outbursts – *the authors*]. Second, there is no rapid variability (in X-rays and in the optical range). Third, an expanding envelope in the radio range is observed that can be explained by ejection of H- and He-rich layers as a result of the thermonuclear explosion (this is confirmed well by appearance of the H and He I lines pedestals in the outburst). According to [19] the hypothesis of a neutron star is not excluded completely.

The known X-ray novae with a black hole companion exhibit the excess of power spectrum in the hard X-ray range and rapid variability of the X-ray flux, which are not observed in CI Cam. Therefore, the probability of black hole presence in CI Cam system is very low. The presence of a normal OB-type star in the system is eliminated in [19], too, because the expected X-ray flux in quiescence is lower by two orders than observed one of CI Cam.

The main conclusions of our study are the following.

(1) The 1100-day cycle of variation in CI Cam was found in photometry as well as in fluxes of some low-excitation emission lines. This cycle may be a consequence of orbital motion in a widely detached system with a giant star and of the reflection effect on its surface.

(2) With our V-band photometry we confirm the $11^d.7$ period found by Miroshnichenko [5] before the 1998 outburst. The model calculations show that this period may be identified with the rotation period of relativistic jets in radio maps. The radio map modelling reveals the following range of parameters: the inclination of the jet's rotation axis to the line of sight $i = (35 - 40^o)$, the angle between the rotation axis and the direction of the jet outflow $\theta = (7 - 10^o)$, and the spatial velocity of the jet of 0.23–0.26c.

(3) The connection between the behaviour of different emission lines and their formation regions is found. Apparently this relation reflects the

star envelope stratification. The rapid variability of emission fluxes of helium and several iron lines is found. Probably, the variability is caused by variations of the X-ray flux in quiescence. The time lag by 50-250 days of the [N II] λ5755Å forbidden line brightening was detected relative to the peak of the outburst in optical, X-ray and radio ranges.

(4) The amplitudes of the outburst in different emission lines were studied. The relation between the amplitude of the flux change in lines and the total line excitation potential was found.

We are grateful to S.A. Pustilnik and A.V. Ugryumov for carrying out observations of CI Cam in the outburst of 1998 during their BTA observing time, to staff members of SAO RAN A.N. Burenkov, G.G. Valyavin, V.V. Vlasyuk, D.N. Monin, and N.I. Serafimovich for their spectral observations of CI Cam. Also, we are thankful to E.A. Karitskaya and S.Yu. Shugarov for their help in photometric observations. The authors thank P. Roche and S.Yu. Shugarov for their opportune information about the CI Cam outburst.

The study has been supported partially by the Federal Scientific and Technical Program "Astronomy" through grant 1.4.2.2. The authors V.P. Goranskij and N.V. Metlova are thankful to this fund for a support.

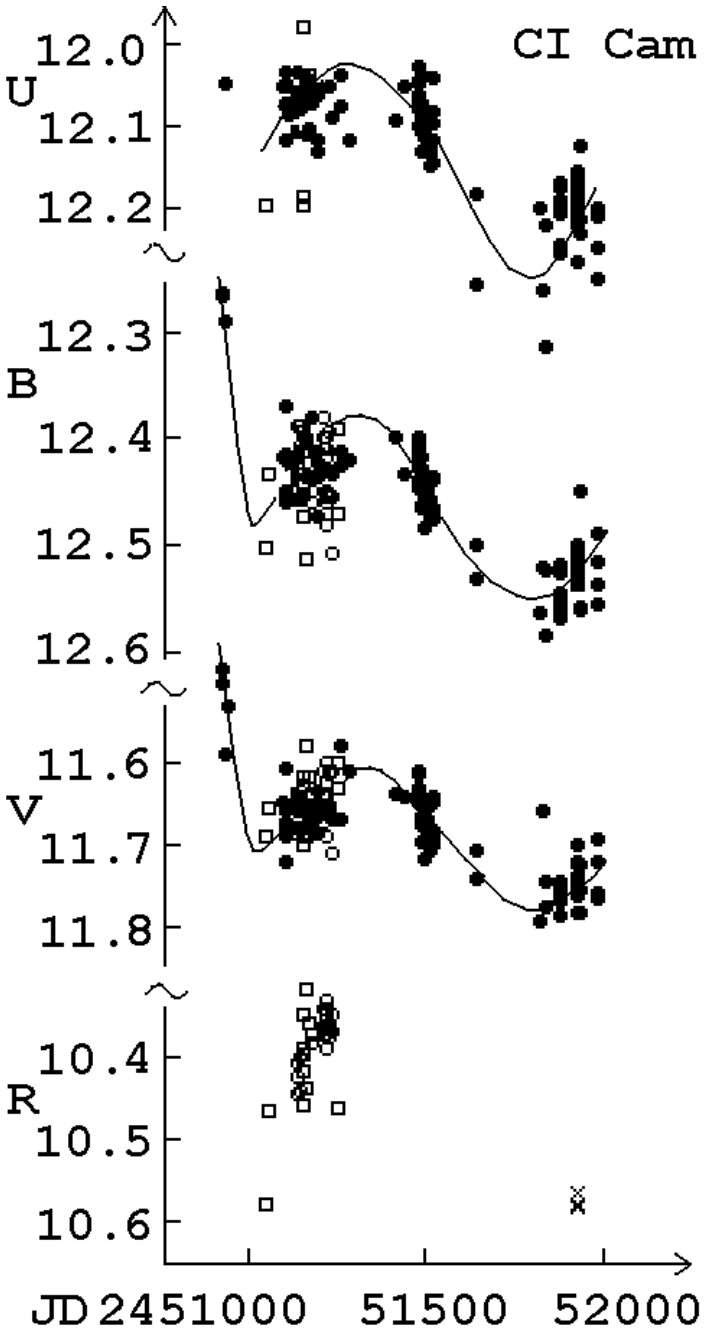

Fig. 1. The light curves of CI Cam in $UBVR$ bands after the outburst in 1998.

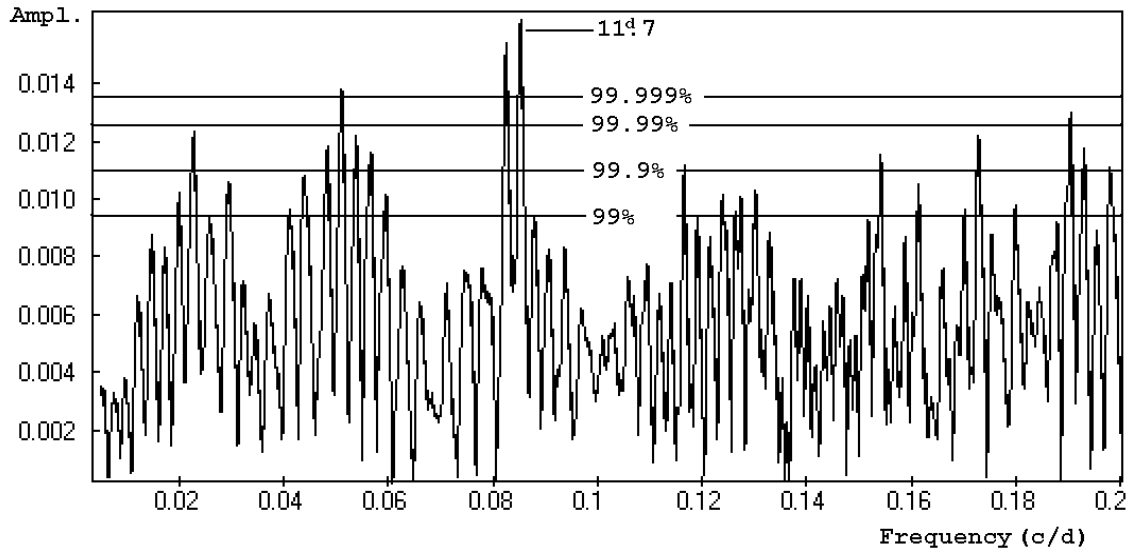

Fig. 2. The amplitude – frequency relation (the amplitude spectrum according to Deeming) for the residuals from the mean light curve with 1100-day period in the V band. The horizontal lines show the significance levels.

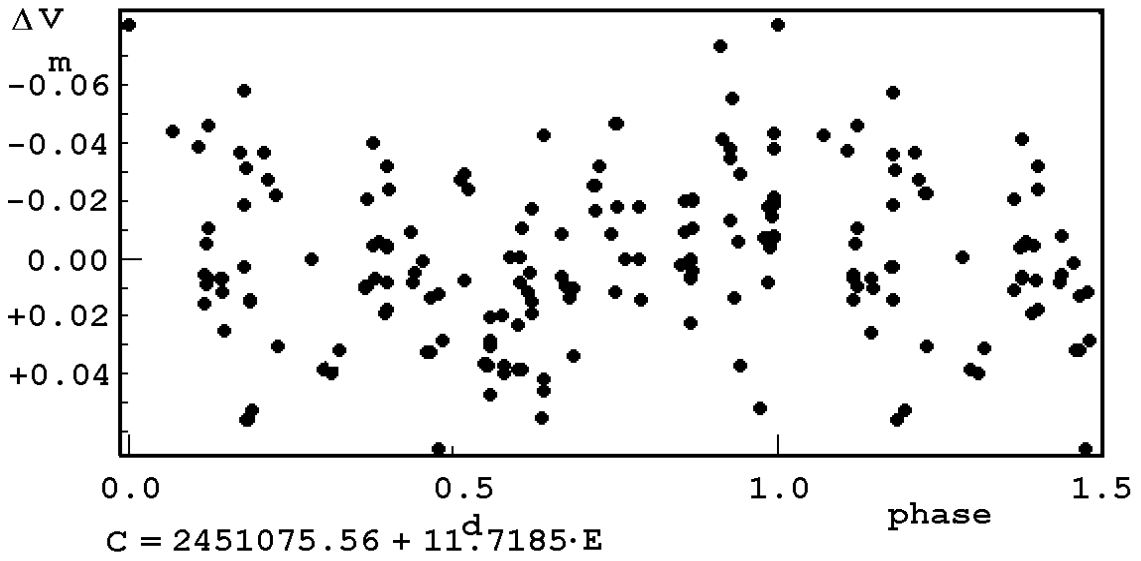

Fig. 3. The V band light curve for the residuals with period 11.72 day.

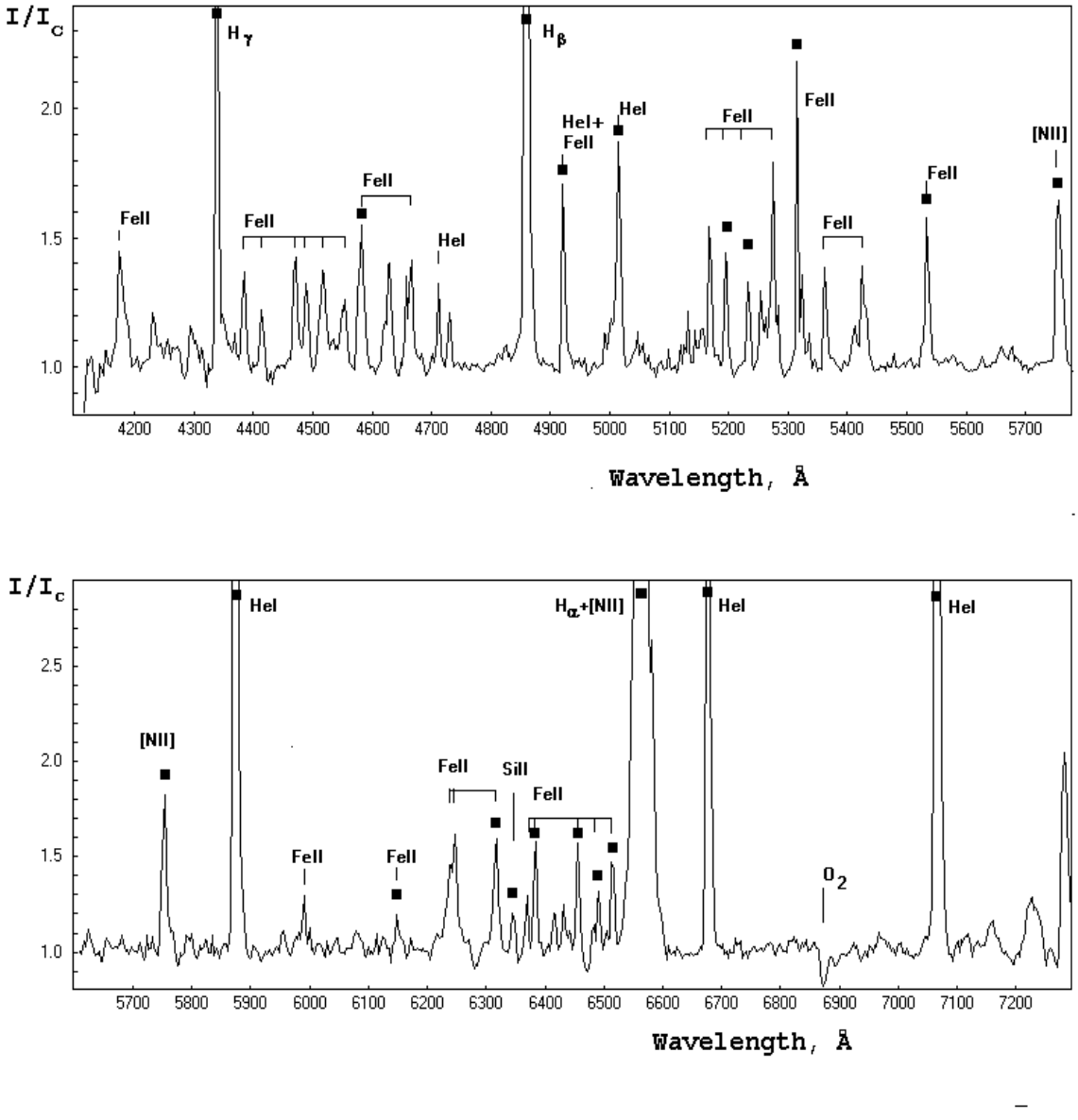

Fig. 4. The quiescent spectrum of CI Cam in the blue (a) and red (b) ranges. The filled squares mark emission lines selected for measurements.

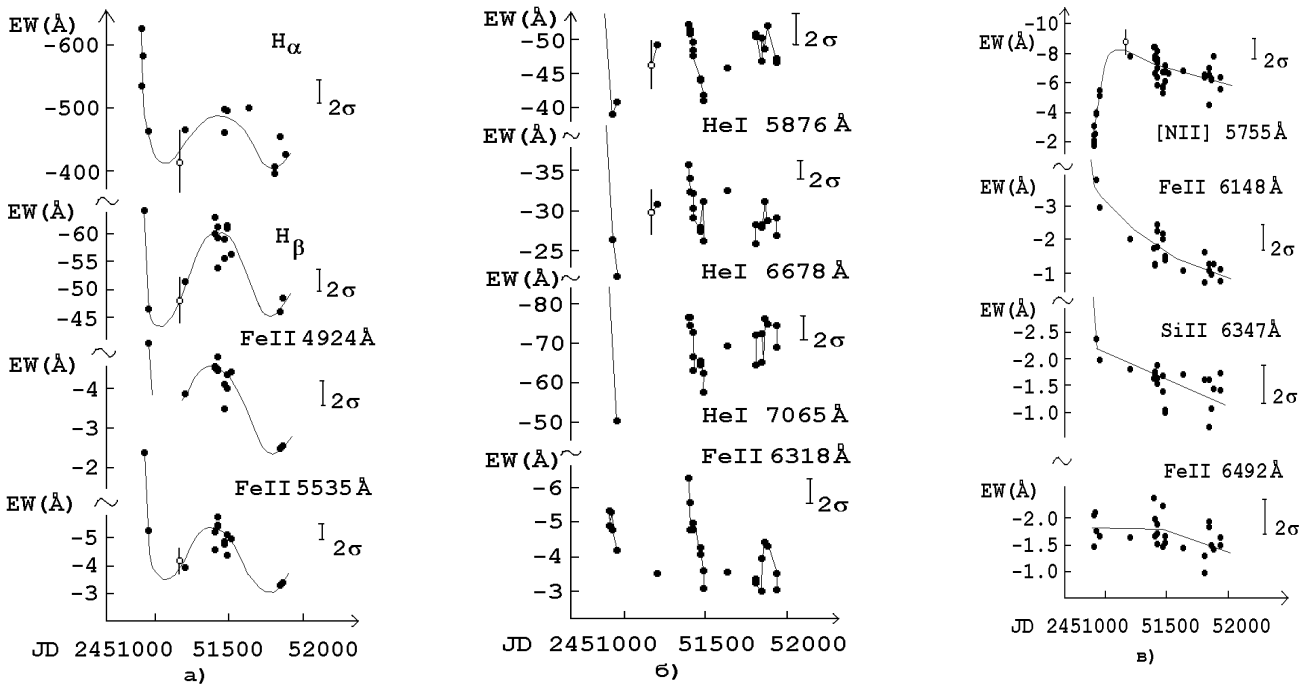

Fig. 5. The relation of equivalent width versus time for some emission lines. Different types of behaviour are shown: (a)–the H_α type; (b)–the He I type; (c, upper curve)–the [N II] type; (c, three lower curves)–the Si II type. The open circles are observations from [19]. The uncertainties of equivalent width determination of 2σ are shown with vertical bars.

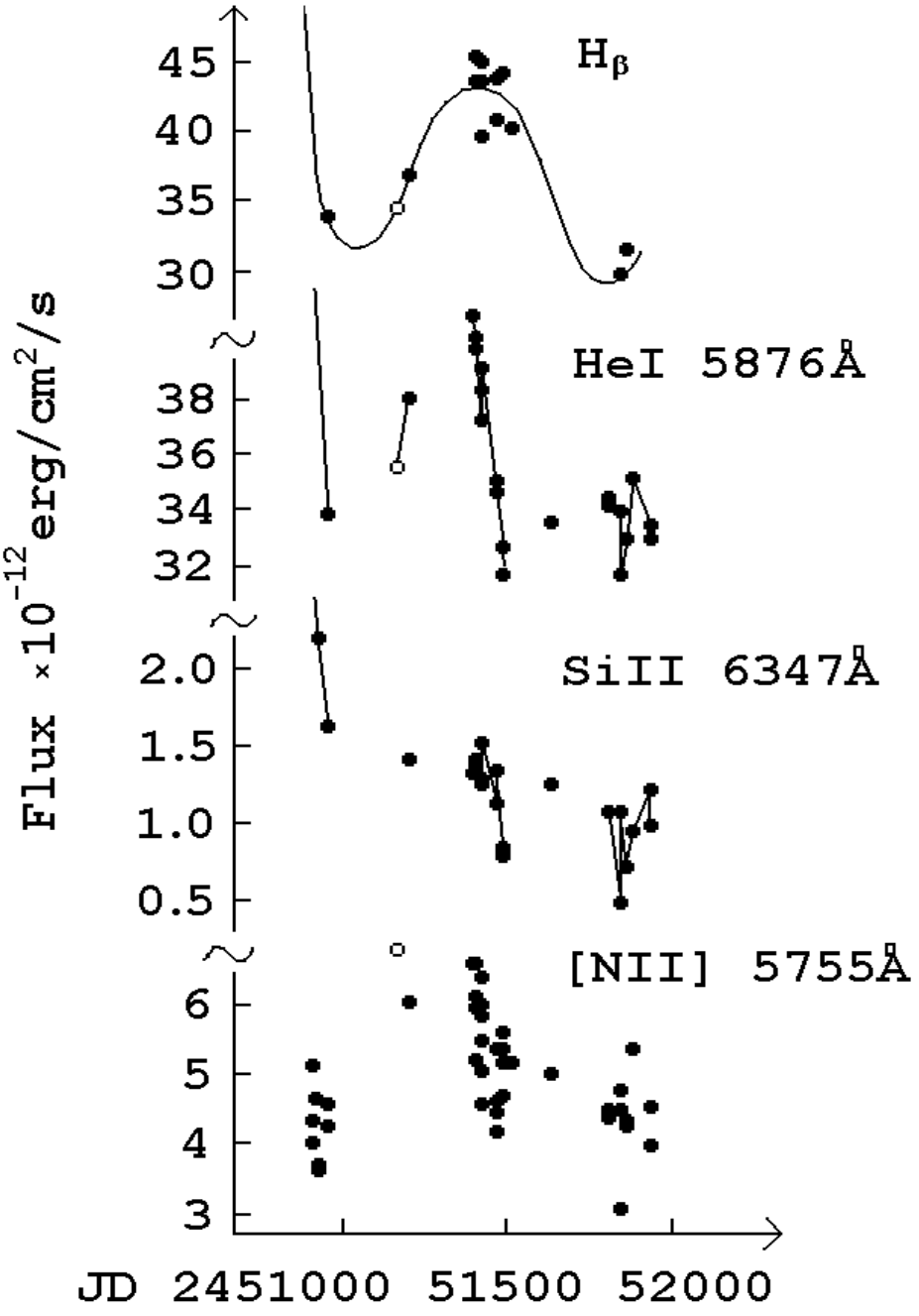

Fig. 6. The relation of fluxes in lines with distinct behaviour types versus time.

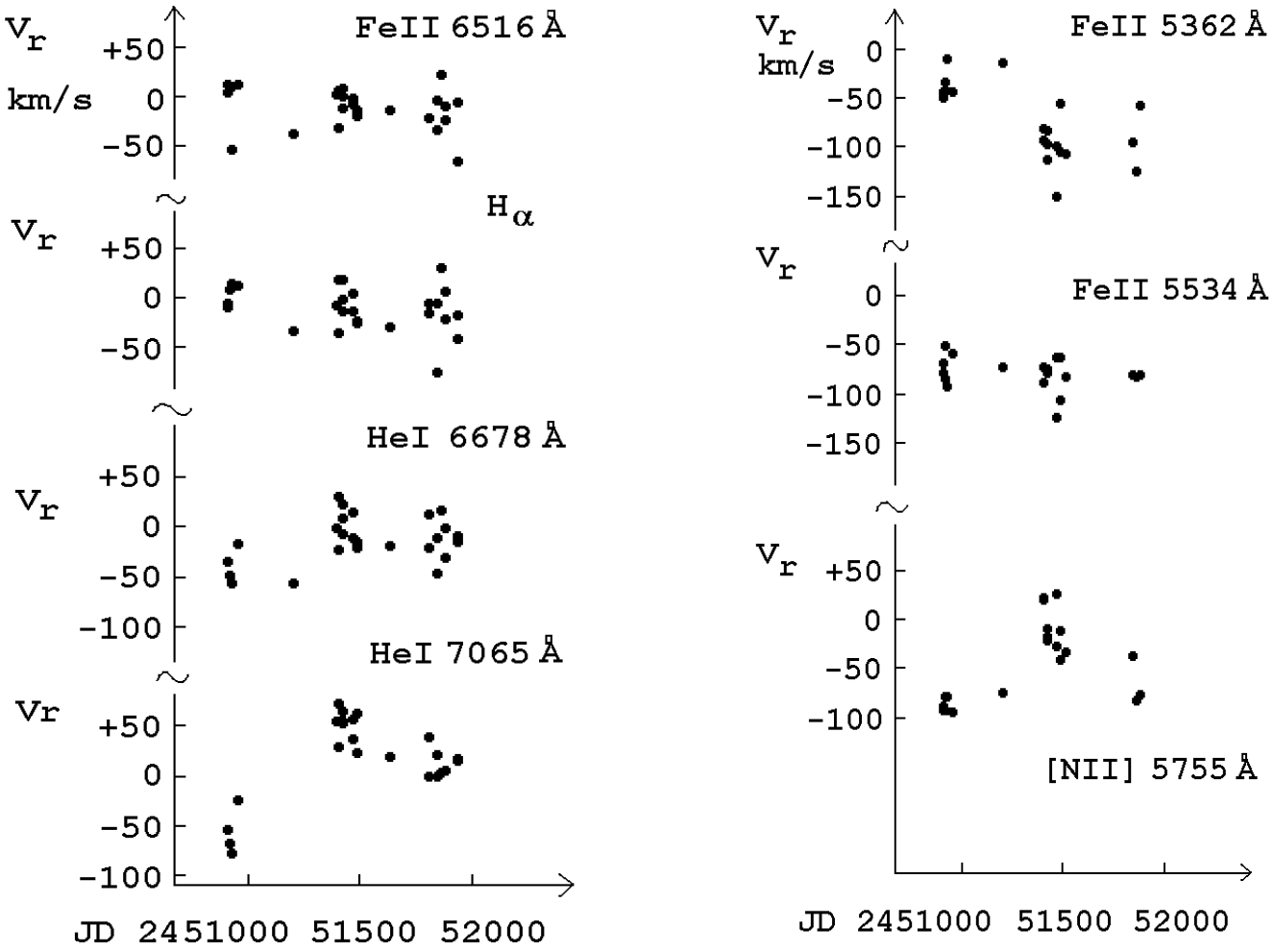

Fig. 7. The radial velocity curves of some emission lines: (a)– in the red spectral range referred to the O_2 λ6872Å absorption band, (b)– in the blue range referred to the [O I] λ5577Å telluric line.

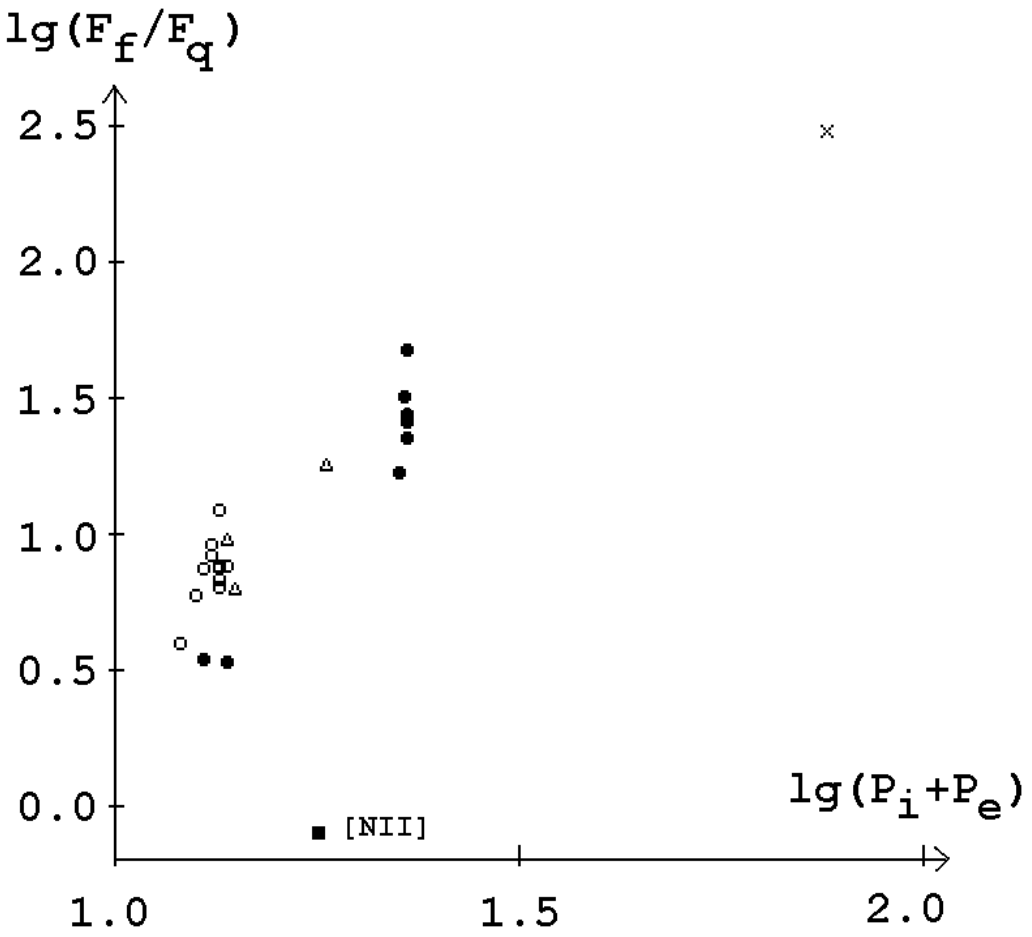

Fig. 8. The dependence between the ratio of the emission line outburst flux (F_f) to its quiescent flux (F_q) and the line's total excitation potential (the sum of ionization P_i and excitation P_e potentials), in the logarithmic scale. The He II λ4686Å line is marked with a cross, He I and Fe II lines of the same behaviour type marked with filled circles, Balmer lines and Fe II lines of H_α-type are marked with open circles, the triangles are the Si II-type behaviour lines, and the filled square is the [N II] λ5755Å line.

Table 1. Photometric observations of CI Cam.

JD hel. 24...	V	B	U	R	Device	Tele-scope	Obser-ver(s)
50907.2757	9.53	10.67	-	7.89	CCD	60	L,G
50908.2659	10.095	10.967	10.607	-	pe	60	L,G,M
50909.2812	10.21	11.38	-	8.66	CCD	60	L,G
50910.2565	10.38	11.33	-	8.84	CCD	60	L,G
50911.2581	10.60	11.57	-	9.11	CCD	60	L,G
50912.2555	10.73	11.68	-	9.25	CCD	60	L,G
50917.2980	11.21	-	-	9.86	CCD	60	L
50918.3140	11.30	-	-	9.93	CCD	60	L
50920.2840	11.344	12.141	11.741	-	pe	60	M
50922.2995	11.385	12.172	11.783	-	pe	60	M
50927.2826	11.438	12.213	11.808	-	pe	60	M
50929.2743	11.488	12.264	11.908	-	pe	60	M
50933.2732	11.504	12.265	11.897	-	pe	60	M
50934.3195	-	-	11.921	-	pe	60	M
50941.2947	11.59	12.29	12.05	-	pe	60	M
50942.2832	11.53	12.38	12.16	-	pe	60	M
51103.4740	11.648	12.418	12.051	-	pe	60	M
51104.5430	11.720	12.461	12.117	-	pe	60	M
51105.4780	11.690	12.450	12.051	-	pe	60	M
51105.4850	11.673	12.461	12.077	-	pe	60	M
51105.4920	11.683	12.458	12.071	-	pe	60	M
51110.5100	11.659	12.414	12.050	-	pe	60	M
51111.5070	11.607	12.369	12.036	-	pe	60	M
51112.3910	11.675	12.422	12.086	-	pe	60	M
51133.2798	11.606	12.410	12.086	-	pe	60	S
51133.2960	11.630	12.398	12.062	-	pe	60	S
51133.3062	11.589	12.408	12.038	-	pe	60	S
51137.4366	11.644	12.417	12.035	-	pe	60	M
51141.3537	11.655	12.416	12.066	-	pe	60	M
51143.3548	11.626	12.398	-	10.407	pe	70	G
51143.3705	11.644	12.434	-	10.424	pe	70	G
51143.3857	11.658	12.468	-	10.443	pe	70	G
51143.3548	11.626	12.398	-	10.407	pe	70	G
51143.3705	11.644	12.434	-	10.424	pe	70	G
51143.3857	11.658	12.468	-	10.443	pe	70	G
51148.3629	11.607	12.398	-	10.398	pe	70	G
51148.3791	11.617	12.417	-	10.440	pe	70	G
51152.3388	11.681	12.457	12.079	-	pe	60	M
51161.3109	11.681	12.435	12.110	-	pe	60	M
51163.5998	11.660	12.435	12.040	-	pe	60	M
51164.4602	11.652	12.399	12.062	-	pe	60	M
51176.2600	11.677	12.436	12.103	-	pe	60	M
51179.3464	11.633	12.460	-	10.380	pe	70	G
51179.3608	11.643	12.470	-	10.370	pe	70	G
51180.2383	11.666	12.379	12.072	-	pe	60	M

Table 1 (continued).

JD hel. 24...	V	B	U	R	Device	Tele-scope	Obser-ver(s)
51197.3893	11.649	12.413	12.055	-	pe	60	M
51197.4001	11.636	12.437	12.131	-	pe	60	M
51199.2277	11.686	12.472	12.116	-	pe	60	M
51199.2378	11.667	12.424	12.061	-	pe	60	M
51213.2166	11.623	12.390	-	-	pe	70	G
51213.2207	11.643	12.410	-	10.360	pe	70	G
51213.2389	11.613	12.410	-	10.370	pe	70	G
51213.2490	11.583	12.420	-	10.340	pe	70	G
51218.2389	11.570	12.459	-	10.362	pe	70	G,K
51218.2464	11.609	12.464	-	10.389	pe	70	G,K
51218.2540	11.631	12.428	-	10.348	pe	70	G,K
51218.2612	11.596	12.463	-	10.354	pe	70	G,K
51223.2283	11.663	12.470	-	10.330	pe	70	G,K
51223.2329	11.663	12.470	-	10.330	pe	70	G,K
51223.2425	11.623	12.410	-	10.340	pe	70	G,K
51223.2529	11.633	12.490	-	10.370	pe	70	G,K
51223.2630	11.613	12.420	-	10.340	pe	70	G,K
51227.2442	11.662	12.431	12.053	-	pe	60	M
51232.2840	11.585	12.404	-	10.365	pe	70	G
51232.2974	11.633	12.465	-	10.373	pe	70	G
51232.3059	11.622	12.441	-	10.358	pe	70	G
51235.3438	11.668	12.433	12.091	-	pe	60	M
51235.3636	11.583	12.464	-	10.347	pe	70	G
51235.3771	11.681	12.517	-	10.369	pe	70	G
51264.3012	11.579	12.413	12.037	-	pe	60	M
51265.2567	11.669	12.426	12.077	-	pe	60	M
51287.2855	11.610	12.420	12.117	-	pe	60	M
51420.5427	11.640	12.400	12.095	-	pe	60	M
51440.5108	11.643	12.433	12.051	-	pe	60	M
51485.5330	11.647	12.429	12.061	-	pe	60	M
51485.5639	11.638	12.421	12.049	-	pe	60	M
51485.5708	11.649	12.429	12.079	-	pe	60	M
51485.5771	11.648	12.438	12.066	-	pe	60	M
51485.5837	11.634	12.418	12.029	-	pe	60	M
51485.5910	11.635	12.406	12.067	-	pe	60	M
51485.5972	11.615	12.417	12.101	-	pe	60	M
51485.6048	11.634	12.447	12.045	-	pe	60	M
51485.6111	11.633	12.400	12.050	-	pe	60	M
51485.6180	11.610	12.417	12.071	-	pe	60	M
51485.6246	11.634	12.416	12.046	-	pe	60	M
51485.6319	11.647	12.441	12.063	-	pe	60	M
51492.4350	11.698	12.466	12.107	-	pe	60	M
51492.4461	11.678	12.449	12.102	-	pe	60	M
51492.4572	11.696	12.463	12.132	-	pe	60	M
51493.5305	11.651	12.418	12.072	-	pe	60	M

Table 1 (continued).

JD hel. 24...	V	B	U	R	Device	Tele-scope	Obser-ver(s)
51493.5371	11.666	12.429	12.039	-	pe	60	M
51493.6246	11.674	12.434	12.095	-	pe	60	M
51493.6322	11.670	12.449	12.107	-	pe	60	M
51499.5344	11.679	12.458	12.085	-	pe	60	M
51499.5414	11.719	12.485	12.114	-	pe	60	M
51502.5240	11.657	12.449	12.102	-	pe	60	M
51502.5313	11.674	12.460	12.097	-	pe	60	M
51502.5386	11.671	12.461	12.102	-	pe	60	M
51514.5609	11.707	12.472	12.132	-	pe	60	M
51514.5679	11.687	12.458	12.150	-	pe	60	M
51525.5179	11.691	12.440	12.040	-	pe	60	M
51525.5249	11.649	12.436	12.084	-	pe	60	M
51525.5315	11.642	12.471	12.097	-	pe	60	M
51526.4565	11.702	12.475	12.144	-	pe	60	M
51526.4631	11.685	12.465	12.118	-	pe	60	M
51645.2979	11.743	12.499	12.185	-	pe	60	M
51645.3048	11.706	12.531	12.295	-	pe	60	M
51822.6055	11.794	12.563	12.200	-	pe	60	M
51831.4368	11.660	12.521	12.301	-	pe	60	M
51836.4257	11.746	12.523	12.220	-	pe	60	M
51842.6180	11.776	12.585	12.370	-	pe	60	M
51842.6246	11.808	12.647	12.506	-	pe	60	M
51882.5555	11.755	12.554	12.244	-	pe	60	M
51882.5625	11.787	12.557	12.256	-	pe	60	M
51882.5694	11.766	12.544	12.170	-	pe	60	M
51882.5760	11.765	12.565	12.207	-	pe	60	M
51882.5829	11.771	12.568	12.197	-	pe	60	M
51882.5895	11.769	12.518	12.191	-	pe	60	M
51882.5965	11.744	12.526	12.177	-	pe	60	M
51925.4042	11.721	12.501	12.157	-	pe	60	M
51925.4118	11.725	12.521	12.180	-	pe	60	M
51926.5173	11.764	12.538	12.196	-	pe	60	M
51926.5260	11.754	12.534	12.268	-	pe	60	M
51927.2860	11.760	12.534	12.188	-	pe	60	M
51927.2920	11.782	12.526	12.166	-	pe	60	M
51928.2664	11.749	12.557	-	10.566	CCD	100	B,G
51928.2674	11.749	12.557	-	10.566	CCD	100	B,G
51929.3068	11.751	12.537	-	10.579	CCD	100	B,G
51930.2810	11.742	12.557	-	10.582	CCD	100	B,G
51932.3709	11.762	12.530	12.187	-	pe	60	M
51932.3782	11.748	12.530	12.222	-	pe	60	M
51932.3851	11.753	12.530	12.187	-	pe	60	M
51932.3914	11.754	12.522	12.191	-	pe	60	M
51932.3987	11.748	12.526	12.178	-	pe	60	M
51932.4053	11.757	12.532	12.212	-	pe	60	M

Table 1 (the end).

JD hel. 24...	V	B	U	R	Device	Tele-scope	Obser-ver(s)
51932.4126	11.742	12.508	12.214	-	pe	60	M
51932.4195	11.737	12.520	12.200	-	pe	60	M
51932.4264	11.701	12.519	12.187	-	pe	60	M
51934.5163	11.785	12.561	12.230	-	pe	60	M
51935.2836	11.757	12.559	12.213	-	pe	60	M
51935.2898	11.726	12.449	12.126	-	pe	60	M

Observers:
B – Barsukova E.A.
G – Goranskij V.P.
K – Karitskaya E.A.(Institute of Astronomy, RAN)
L – Lyuty V.M.
M – Metlova N.V.
S – Shugarov S.Yu.(SAI)

Telescopes:
60 – 60-cm Zeiss reflector of SAI Crimean station;
70 – 70-cm reflector of SAI in Moscow;
100– 100-cm Zeiss reflector of SAO RAN.

Devices:
CCD – CCDs SBIG ST-6 and Electron-K585 (see text);
pe – photoelectric one-channell UBV- and BVR- photometers (see text).

Table 2. Spectral observations.

JD hel. 24...	Date	Range (Å)	Resolution(Å)	Number of sp.	Telescope	Observers
50908.259	1998.04.04	3800-6100	4	2	6-m	P,U
50908.260	1998.04.04	5000-7400	4	1	6-m	P,U
50909.176	1998.04.05	5000-7400	4	1	6-m	P,U
50909.20	1998.04.05	3800-6100	4	1	6-m	P,U
50910.20	1998.04.06	3800-6100	4	2	6-m	P,U
50910.205	1998.04.06	5000-7400	4	3	6-m	P,U
50923.25	1998.04.19	3800-6100	7	29	6-m	P,U,M
50923.266	1998.04.19	5000-7400	7	2	6-m	P,U,M
50950.30	1998.05.16	3800-6100	4	2	6-m	V1,F
50950.314	1998.05.16	5000-7400	4	2	6-m	V1,F
51204.333	1999.01.25	3800-6100	4	100	6-m	B1,V1,M,F
51206.30	1999.01.27	5000-7700	0.23	3	6-m	B1,M
51398.534	1999.01.08	5580-7320	4	2	1-m	B2
51399.538	1999.08.09	4100-5800	4	2	1-m	B2
51399.525	1999.08.09	5580-7290	4	2	1-m	B2
51400.510	1999.08.10	4100-5800	4	4	1-m	B2
51400.531	1999.08.10	5600-7300	4	4	1-m	B2
51423.551	1999.09.02	5590-7330	4	4	1-m	B2
51423.566	1999.09.02	4100-5780	4	3	1-m	B2
51424.551	1999.09.03	4100-5780	4	4	1-m	B1,B2
51425.581	1999.09.04	5600-7300	4	13	1-m	B1,B2
51426.519	1999.09.05	4100-5780	4	3	1-m	B1,B2
51426.561	1999.09.05	5600-7300	4	5	1-m	B1,B2
51464.523	1999.10.13	5600-7320	4	6	1-m	B3
51464.542	1999.10.13	4100-5780	4	4	1-m	B3
51465.434	1999.10.14	4100-5780	4	4	1-m	B3
51465.458	1999.10.14	5600-7320	4	6	1-m	B3
51485.653	1999.11.03	4100-5700	4	3	1-m	B2
51485.666	1999.11.03	5670-7340	4	4	1-m	B2
51488.416	1999.11.06	5670-7320	4	6	1-m	B2
51488.447	1999.11.06	4100-5780	4	6	1-m	B2
51514.288	1999.12.01	4100-5780	4	10	1-m	B2,B3
51635.187	2000.03.31	5660-7330	4	10	1-m	B2
51810.552	2000.09.23	5600-7280	4	5	1-m	V2
51812.555	2000.09.25	5600-7230	4	10	1-m	S
51844.500	2000.10.27	4100-5800	4	11	1-m	B2
51846.430	2000.10.29	5600-7240	4	5	1-m	V2
51848.416	2000.10.31	5600-7300	4	6	1-m	B2
51864.375	2000.11.16	5660-7320	4	9	1-m	B2
51864.448	2000.11.16	4100-5780	4	10	1-m	B2
51880.312	2000.12.01	5660-7330	4	17	1-m	B2
51885.319	2000.12.06	4500-7000	5	164*)	6-m	V1,M,F
51936.243	2001.01.26	5660-7320	4	10	1-m	B2
51937.234	2001.01.27	5660-7320	4	4	1-m	V2

*) aperture spectra through cirri.

Observers:

B1 – Barsukova E.A.	M – Monin D.N.	V1 – Valyavin G.G.
B2 – Borisov N.V.	P – Pustilnik S.A.	V2 – Vlasyuk V.V.
B3 – Burenkov A.N.	S – Serafimovich N.I.	U – Ugryumov A.V.
F – Fabrika S.N.		

Telescopes:
6-m – 6-meter reflector BTA;
1-m – 1-m Zeiss reflector SAO RAN.

Table 3.
The behaviour of emission lines in the outburst.

Line	$\lambda_{lab.}$	EW_f/EW_q	$log(F_f/F_q)$	$log(P_i+P_e)(EV)$	Type
H_γ	4340.468	4.86	0.96	1.12	H_α
FeII	4414.78	2.97	0.80	1.13	H_α
HeI	4471.688	12.28	1.43	1.36	HeI
FeII	4583.290	2.89	0.88	1.13	H_α?
HeII	4685.810	132.82	2.49	1.88	$HeII$
H_β	4861.332	3.24	0.87	1.11	H_α
HeI(+FeII)	4921.929	3.79	1.51	1.36	HeI
HeI	5015.675	22.90	1.68	1.36	HeI
FeII	5197.569	3.49	0.92	1.12	H_α
FeII	5234.620	5.52	1.09	1.13	H_α
FeII	5316.609	2.90	0.87	1.13	H_α
FeII	5534.860	2.70	0.83	1.13	H_α
$[NII]$	5754.640	0.32	-0.10	1.25	$[NII]$
HeI	5875.792	8.70	1.35	1.36	HeI
FeII	6147.735	2.60	0.98	1.14	$SiII$
FeII	6318.000	1.23	0.53	1.14	HeI
SiII	6347.091	5.52	1.26	1.26	$SiII$
FeII	6385.470	1.00	0.54	1.11	HeI
FeII	6456.376	1.71	0.88	1.14	H_α
FeII	6491.670	0.94	0.82	1.13	$SiII$
FeII	6516.053	1.88	0.77	1.10	H_α
H_α	6562.816	1.21	0.60	1.08	H_α
HeI	6678.151	7.92	1.41	1.36	HeI
HeI	7065.440	4.60	1.23	1.36	HeI

References

1. Lamers H.J.G.L.M., Zickgraf F.-J., de Winter D., et al.,// Astron. and Astrophys. 1998. V.340. P.117.
2. Merrill P.W., Humasson M.L., Burwell C.G.//Astrophys. J. 1932. V.76, P.156.
3. Merrill P.W., Burwell C.G.//Astrophys. J. 1933. V.78, P.97.
4. Downes R.A. //Publ. Astron. Soc. Pacific. 1984. V.96, P.807.
5. Miroshnichenko A.S. //Astron. and Astrophys. Trans. 1995. V.6, P.251.
6. Bergner Yu.K., Miroshnichenko A.S., Yudin R.V., Kuratov K.S., et al.//Astron. and Astrophys. Suppl. Ser. 1995. V.112. P.221.
7. Miroshnichenko A.S.//Odessa Astron. Publ. 1994. V.7. P.76.
8. Chkhikvadze Ya.N.// Astrofizika. 1970. V.6. P.65.
9. Smith D., Remillard R., Swank J., et al.//IAU Circ. 1998. No. 6855.
10. Belloni T., Dieters S., van den Ancker M.E., Fender R.P. et al.// Astrophys. J. 1999. V.527. P.345.
11. Ueda Y., Ishida M., Inoue H. et al.//Astrophys. J. 1998. V.508. L167.
12. Robinson E.L., Welch W.F., Adams M.T., Cornell M.E.//IAU Circ. 1998. No.6862.
13. Barsukova E.A., Fabrika S.N., Pustilnik S.A., Ugryumov A.V.// Bull. Spec. Astrophys. Obs. 1998, V.45, P.145.
14. Clark J.S., Steele I.A., Fender R.P., Coe M.J.// Astron. and Astrophys. 1999. V.348. P.888.
15. Barsukova E.A., Fabrika S.N.// Variable star as a clue to understanding the structure and evolution of Galaxy. 2000. Ed. N.N.Samus and A.V.Mironov, Cygnus. Nizhny Arkhys. P.154.
16. Clark J.S., Miroshnichenlo A.S., Larionov V.M., et al.,// Astron. and Astrophys.. 2000. V.356. P.50.
17. Hjellming R.M., Mioduszewski A.J.//Sky and Telescope. 1998. V.96. No.2. P.22.
18. Hjellming R.M., Mioduszewski A.J.//IAU Circ. 1998. No.6872.
19. Orlandini M., Parmar A.N., Frontera F., et al.//Astron. and Astrophys. 2000. V.356. P.163.
20. Parmar A.N., Belloni T., Orlandini M., et al.// Astron. and Astrophys. 2000. V.360. L.31.
21. Kornilov V.G., Volkov I.M., Zakharov A.I., et al.// Sternberg Institute Trans. 1991. V.63.
22. Garsia M.R., Berlind P., Barton E., McClintock J.E.// IAU Circ. 1998. No.6865.
23. Hynes R.I., Roche P., Haswell C.A., et al.//IAU Circ. 1998. No.6871.
24. Deeming T.J.// Astrophys. Space Sci. 1975. V.36. P.173.
25. Kato T., Uemura M.//Inform. Bull. Var. Stars. 2001. No.5081.

26. Chentsov E.L., Klochkova V.G., Tavolganskaya N.S.// Bull. Spec. Astrophys. Obs. 1999. V.48. P.21.

27. Striganov A.R., Sventitskii N.S.// Tables of spectral lines of the neutral and ionized atoms. Atomizdat. M. 1966.

28. Heung S., Aller L.H., Feibelman W.A. et al.//Monthly Notices Roy. Astron. Soc. 2000. V.318. P.77.

29. Meinel A.B., Aveni A.F., Stockton M.W.//Catalog of emission lines in astrophysical objects. Ed.II. 1969. Tucson, Univ. of Arizona.

30. Iben I.//Astrophys. J. 1982. V.259. P.244.